Plasmonics
https://doi.org/10.1007/s11468-020-01247-y

# Microring Plasmonic Transducer Circuits for Up-Downstream Communications

M. Bunruangses[1] · P. Youplao[2,3] · I. S. Amiri[4] · N. Pornsuwancharoen[5] · S. Punthawanunt[6] · P. Yupapin[2,3]

Received: 14 September 2019 / Accepted: 29 July 2020


## Abstract

The microring circuit is designed to form the upstream and downstream quantum communications. There are one space and two-time functions applied to form the transmission. A circuit consists of 3 microring resonators, where there are three processes of each transmission. Firstly, the space function pulse (soliton) fed into the system via the main ring input port. The whispering gallery mode (WGM) is generated at the center ring with suitable parameters. The dipole oscillation is formed by the coupling between plasmonic wave and gold grating, which will change in the dipole oscillation frequency inducing the change in the plasmonic sensor. The flip-flop signals obtained from the bright and dark soliton via the throughput and drop ports can apply for the transmission clock signals. Secondly, the quantum codes formed by a time-energy function input into the system via a silicon ring, which induced the four-wave mixing induced by the coherent light in a ***GaAsInP*** ring, can be identified and the quantum bits(qubits) formed by the polarized signal orientation. The quantum information is multiplexed into the system. Thirdly, the carrier time function will input via the add port main ring. By using the resonant condition, the multiplexed signals of those processes will transmit via either WGM or throughput port for wireless or cable transmission, respectively. The downstream process is processed the same way as the upstream, where the multiplexer is placed by the de-multiplexer. By varying the input power, the manipulation result has shown the potential realistic application for quantum and telepathic communications.

**Keywords** Plasmonic sensors · Plasmonic transducer · Quantum communication · Telepathic communication

## Introduction

Silicon microring resonator has been the promising devices for various applications [1–4], where the key advantages are small size fabrication ability and flexible applications. It can apply in various forms of the devices [5–8], where one of them is the electro-optic signal conversion. The photon aspect of light can apply for a quantum device, which is known as a photonic device. The optical (electrical) and photonic signal conversion can be converted and use for various forms [9,

✉ P. Youplao
phichai.youplao@tdtu.edu.vn

✉ P. Yupapin
preecha.yupapin@tdtu.edu.vn

M. Bunruangses
montree.b@rmutp.ac.th

I. S. Amiri
amiri@bu.edu

N. Pornsuwancharoen
nithiroth.po@rmuti.ac.th

S. Punthawanunt
suphanchai.pun@kbu.ac.th

[1] Department of Computer Engineering, Faculty of Industrial Education, Rajamangala University of Technology Phra Nakhon, Bangkok 10300, Thailand

[2] Computational Optics Research Group, Advanced Institute of Materials Science, Ton Duc Thang University, District 7, Ho Chi Minh City, Vietnam

[3] Faculty of Applied Sciences, Ton Duc Thang University, District 7, Ho Chi Minh City, Vietnam

[4] Division of Materials Science and Engineering, Boston University, Boston, MA 02215, USA

[5] Department of Electrical Engineering, Faculty of Industry and Technology, Rajamangala University of Technology Isan, Sakon Nakhon Campus, Sakon Nakhon 47160, Thailand

[6] Multidisciplinary Research Center, Faculty of Science and Technology, Kasem Bundit University, Bangkok 10250, Thailand

Published online: 26 August 2020

10]. The main objective to confirm the quantum behavior within the microring device is the nonlinear property called a four-wave mixing [11], which can be used to form the quantum entangled bits within the nonlinear microring resonator. In this article, the Drude model of the coupling between the plasmonic wave and metal surface known as a polariton was employed to form the plasmonic sensor and dipole oscillation [12]. By using the space and time (space-time) multiplexing functions, the combined pressure sensor, quantum code, and flip-flop(clock) signals with carrier signals can form the transmission in either wireless or cable link. The space function signal is the spatial soliton pulse, which fed into the microring circuits via the input port. The induced voice signals from the plasmonic sensor were modulated by the first time function input via the add port, where the signals were multiplexed by higher frequency signals and circulated within the system. By using the flip-flop switching control (clock) [13], the resonant multiplexed signals transmit to the end users in either cable or wireless (Light Fidelity, LiFi) link [14]. The downstream transmission can perform similarly with the upstream system. The full duplex of the transmission is also available from both ends. In application, the second time function is input by the high frequency (energy) function, which is known as the spiritual (time-energy) function [15]. It has the quantized energy in the form of the polarized entangled photons, which means that the solid angle of the output can form by the wave-particle propagation called time tunnel (wormhole). It confirms that the time tunnel can establish in both locations of the telephone link.

## Background

The required output of the system is the whispering gallery mode at the center microring resonator. The used parameters are based on the fabrication parameters, where the ring radius is ranged from 1 to 10 μm [16, 17]. In the simulation, the used parameters are based on realistic fabrication parameters [4, 6]. The silicon microring circuit model is the resonating system shown in Fig. 1. The proposed nonlinear microring circuits configured to form the upstream quantum communication, which is a capability fabrication structure. The suitable input power and space function signal (soliton) is applied to the circuit, where the WGM outputs for plasmonic dipole oscillation areobtained. Other parts of the system are plasmonic transducer mechanism, four-wave mixing, and transmission given by the following.

### Plasmonic Transducer

A soliton is applied to form the space-function of one dimension, and propagate in the z-direction as [18, 19].

$$S(z,t) = \boldsymbol{A}\mathbf{sech}\left[\frac{\boldsymbol{T}}{\boldsymbol{T_0}}\right]\left[\boldsymbol{e}^{\left[\frac{z}{2L_D}\right]}\right] \tag{1}$$

where the phase term and the dispersion of a soliton pulse are included in the simulation. The other parameters of soliton can be considered as in [19].

By using the Drude model, the plasma wave frequency is produced by the plasmonic wave on the surface of the used metal and is related to the change between the polariton wave frequency and electric power, where the mechanism of the transducer as in this case can be described by [12, 20].

$$\boldsymbol{\epsilon}(\boldsymbol{\omega}) = \mathbf{1} - \frac{\boldsymbol{ne^2}}{\boldsymbol{\epsilon_0 m \omega^2}} \tag{2}$$

where the relative permittivity, the electron density, the electron charge, the mass, and the angular frequency are represented by $\epsilon_0$, $n$, $e$, and $m$, respectively. The angular frequency, represented by $\omega$, is at the resonant frequency, $\omega_p$, called the plasma frequency.

The sign of the dielectric function changes from negative to positive and of which the real part changes to zero, where the plasma resonant frequency can be expressed by

$$\boldsymbol{\omega_p} = \left[\frac{\boldsymbol{ne^2}}{\boldsymbol{\epsilon_0 m}}\right]^{-1/2} \tag{3}$$

The plasmonic wave caused by an electrical field oscillates in parallel to the direction of wave propagation (longitudinal wave). The TM-polarization and the exponential decay of the electrical field can be obtained using the Maxwell equations. The wavelength of the input light signal that propagates to the gold grating is $\lambda$. The resonant wavelength related to the Bragg wavelength is given by $\boldsymbol{\lambda_B} = 2\boldsymbol{n_e}\boldsymbol{\Lambda}$, where $\boldsymbol{n_e}$ is the effective refractive index of the grating and $\boldsymbol{\Lambda}$ is the grating period.

### Four-Wave Mixing

The photon oscillation in the time given by

$$\boldsymbol{B}.\boldsymbol{e}^{-i\omega_2 t_2} \tag{4}$$

where $\omega_2 t_2 = 2\pi\gamma_2 t_2$. The angular frequency is $\omega_2$, the linear frequency is $\gamma_2$, the time is $t_2$, and a constant value is B. The nonlinear effect, known as the Kerr effect, will cause the four-wave mixing to occur in the waveguide. The Kerr effect is a change in the refractive index of the material in response to an applied electric field, of which the relationship is $n = n_0 + n_2 I = n_0 + n_2 P/A_{eff}$, where the linear and nonlinear refractive index of the waveguide material is represented by $n_0$ and $n_2$, respectively. The intensity and the power of the optical signal are represented by $I$ and $P$, respectively. The effective mode core area of the microring resonator waveguide is represented by $A_{eff}$, where most of which range from 0.1 to 0.50 $\mu m^2$.

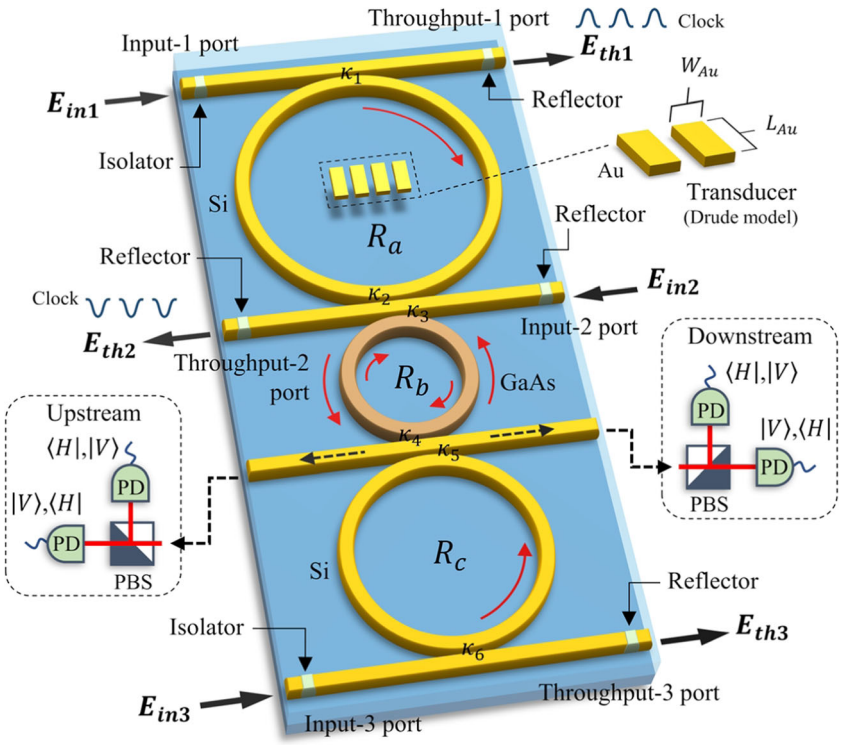


**Fig. 1** Proposed microring circuit for up-downstream link, where $R_a$, $R_b$, and $R_c$ are the radius of the top, center and bottom rings, respectively. $E_{in}$ and $E_{th}$ are the optical fields each at the input and throughput ports, respectively. $\kappa_s$ are the coupling coefficients. The optical isolator and reflector are applied to protect the feedback and filtering outputs, respectively. <H and V> are the horizontal and vertical polarization components

## Transmission

The transmission signals of the system in Fig. 1 are given by

$$\Psi(z,t) = \bar{\mathrm{A}}\ \mathbf{sech}\left[\frac{T}{T_0}\right]\left[e^{\left[\frac{Z}{2L_D}-i(\varphi_1+\varphi_2)t\right]}\right] = \mathrm{A}e^{-i\left(\varphi_1+\frac{E_n}{n\hbar}\right)t} \quad (5)$$

where $A = \bar{\mathrm{A}}\ \mathrm{sech}\left[\frac{T}{T_0}\right]\exp\left(\frac{Z}{2L_D}\right)$, $\varphi_1 = 2\pi\gamma_1 t$ is the phase of the time-multiplexing function, $\varphi_2(t) = \frac{E_n}{n\hbar}$, $\omega_2 = 2\pi\gamma_2 = \frac{E_n}{n\hbar} = \mathrm{nh}\nu$, and $n = 1, 2, 3\ldots$ . The circuit uses a synchronous multiplexing scheme. The optical field inputs are simultaneously fed into the system. The time ($t$) is applied to form the spin projection. The transmission output signals can be detected at each system port. The WGM output signals can be applied to the downstream as well. The optical filter and demultiplexer can be employed to obtain the required signals at the specified device ports.

## Results and Discussion

In a simulation, microring resonators have been arranged to form the proposed circuit, as shown in Fig. 1. Three input space-time function sources with wavelengths of 1.55, 0.60, and 1.40 micrometers are simultaneously fed into the system [21, 22], from which the space-time function multiplexing formed. The upstream signals are now ready for transmission, which are the

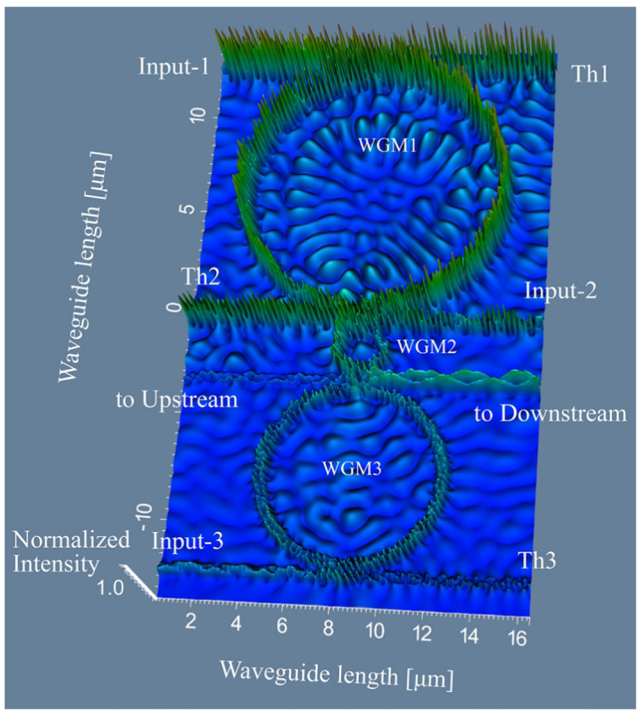


**Fig. 2** The plot of graphical results obtained by the Opti-wave program. The whispering gallery mode (WGM) is generated at the center rings of the circuit, which will be coupled to the gold gratings. The used parameters are $R_a$ = 6.0 μm, $R_b$ = 1.0 μm, $R_c$ = 4 μm, each $\kappa$ = 0.5, Input-1 = Input-2 = Input-3 = 10 mW, with the center wavelength of 1.55 μm, 1.40 μm, and 0.60 μm, respectively. The waveguide loss is 0.1 dBmm$^{-1}$, and the effective core area is 0.25 μm$^2$. The waveguide's refractive indexes are as follows: Si: $n_{Si}$= 3.47 and GaAs: $n_0$= 3.14, $n_2$= $1.3 \times 10^{-13}$ m$^2$W$^{-1}$ [23]

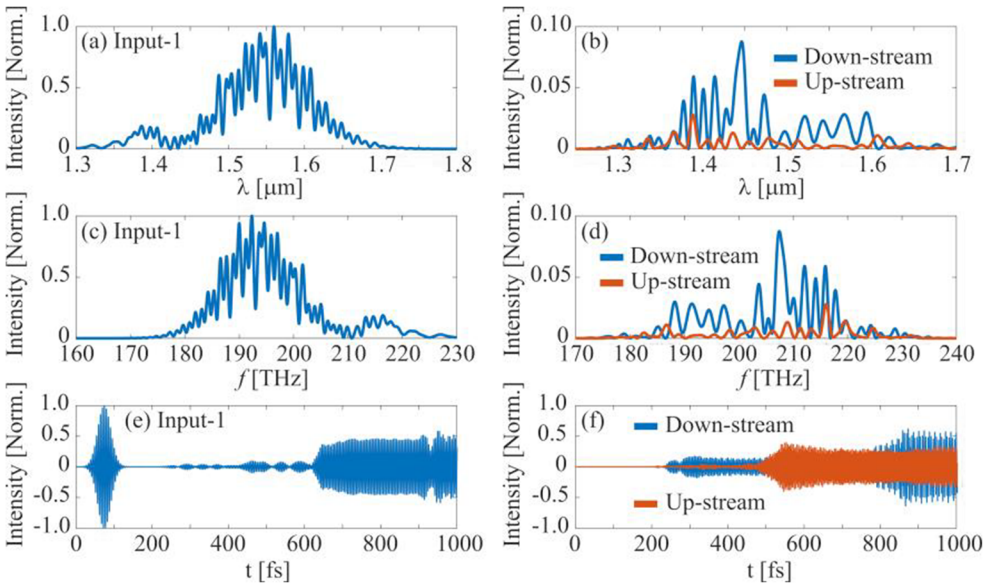


**Fig. 3** The plot of the MATLAB program, where (**a**) Input-1 port from soliton and quantum signals, wavelength, frequency, and time signals; (**b**) throughput-1 and throughput-2 port; (**c**) Input-2 and Input-3; and (**d**) WGM1 and WGM2, with wavelength, frequency, and time

synchronous clock using bright and dark solitons from the throughput and drop port outputs and the quantum bit identification from the time function input source. By using the graphical method, the suitable parameters give the required results at the resonant condition, from which the simulation time is 20,000 round trips. The selected parameters are given in the related figure captions. The MATLAB results are plotted for further discussion. Graph of the Optiwave program using the selected parameters of the resonant system is shown in Fig. 2, where all required information of the system transmission are obtained. The clock and qubit signals are formed, from which the transmission signals are confirmed by the referencing states. The clock signals are generated by the space function pulse, while the entangled photons are established by the polarization orientation of the four-wave mixing signals. The other related signals are detected at each system port, and the WGM outputs are shown in Fig. 3, 4, 5, 6. The WGM beam is generated by the main ring and coupled with

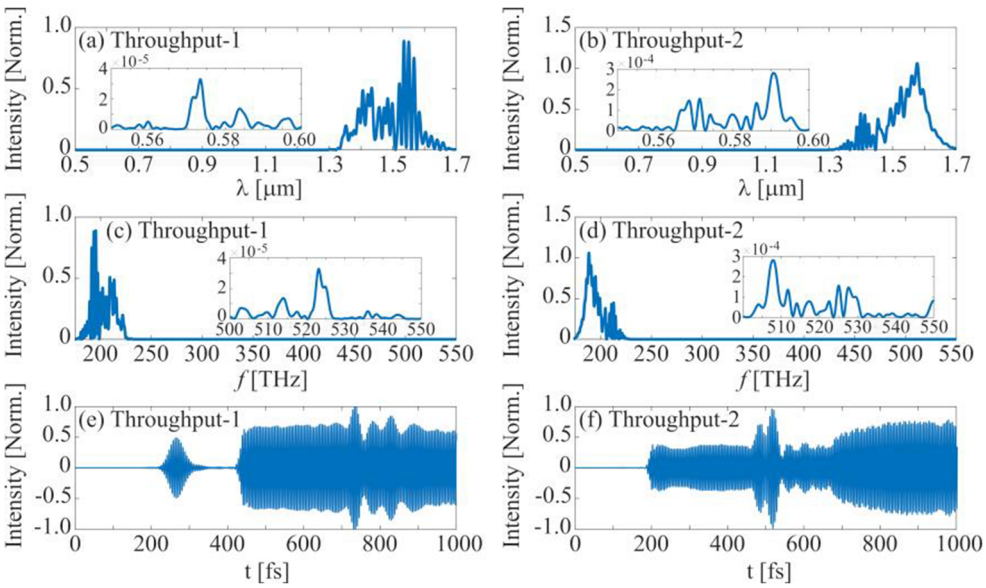


**Fig. 4** The simulation result of MATLAB program, where (**a**) FWM result of WGM2, (**b**) dark at Th-1 and bright at Th-2, (**c**) Clock result of Th-2, and (**d**) Clock result of Th-1

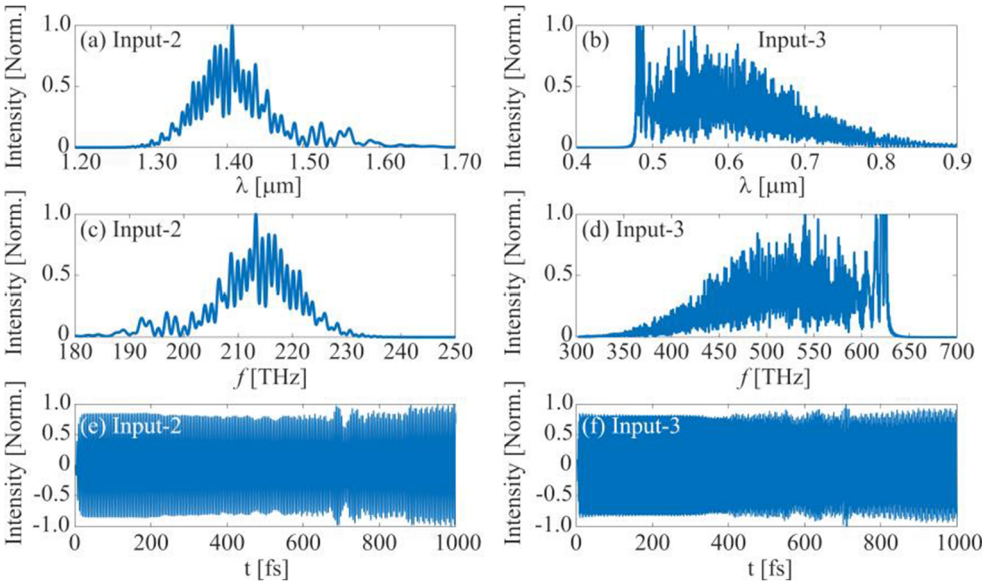


**Fig. 5** The plot results obtained by the MATLAB program, where (**a**) WGM1, (**b**) WGM2, (**c**) throughput-1, and (d) throughput-2, with the changes in input soliton power for sensor investigation

the gold grating, where the plasmonic wave oscillation is known as a polariton wave. The collision of the plasmonic waves introduced the dipole oscillation, where the antenna propagation at Bragg wavelength and the specific frequency occurred. The induced change from the external stimuli to the antenna propagation will change the system output signals, which can be detected and characterized. The multi qubits are also available for continuous-variable quantum key distribution by using the broad spectrum of the four-wave mixing output. The transducer signals, for instance, pressure wave disturbance, can multiplex to the carrier and transmit. The other required sensors related to the plasmonic sensor mechanism can also be applied. The required information can be modulated and multiplexed to the carrier time function, in which more information can be added via the add port. The required signals can retrieve by the specific codes to the downstream side. Four-wave mixing, clock, and WGM signals are shown in Fig. 7. The plasmonic sensor sensitivity graph is shown in Fig. 8, which confirmed the induced change to the transducer observed and interpreted, especially for quantum telephone and communication purposes [24]. In the applications, the flip-flop signals are obtained from the

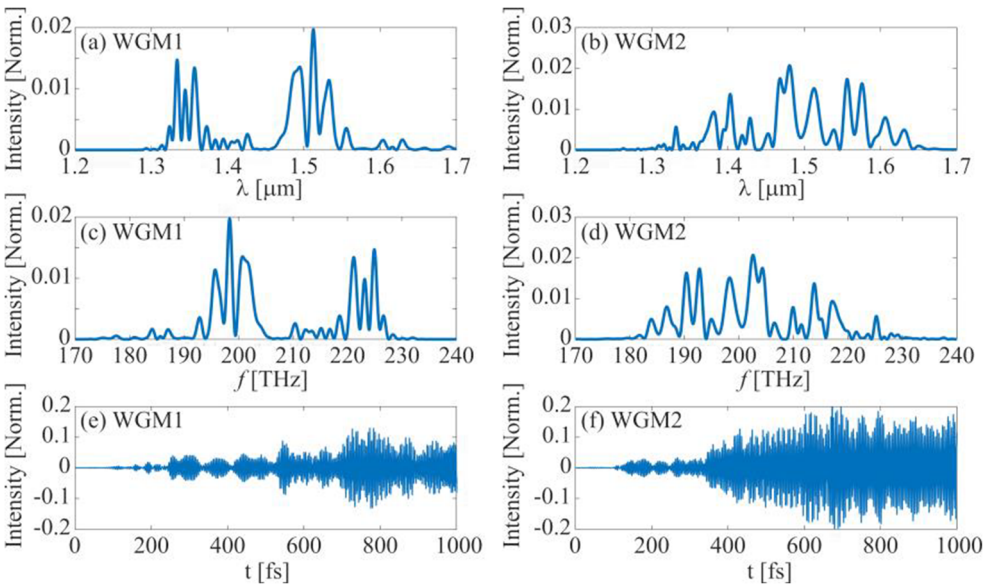


**Fig. 6** The plot of the MATLAB program, the WGM1 and WGM2 signals, where (**a**) and (**b**): wavelength, (**c**) and (**d**): frequency, and (**e**) and (**f**): time signals.

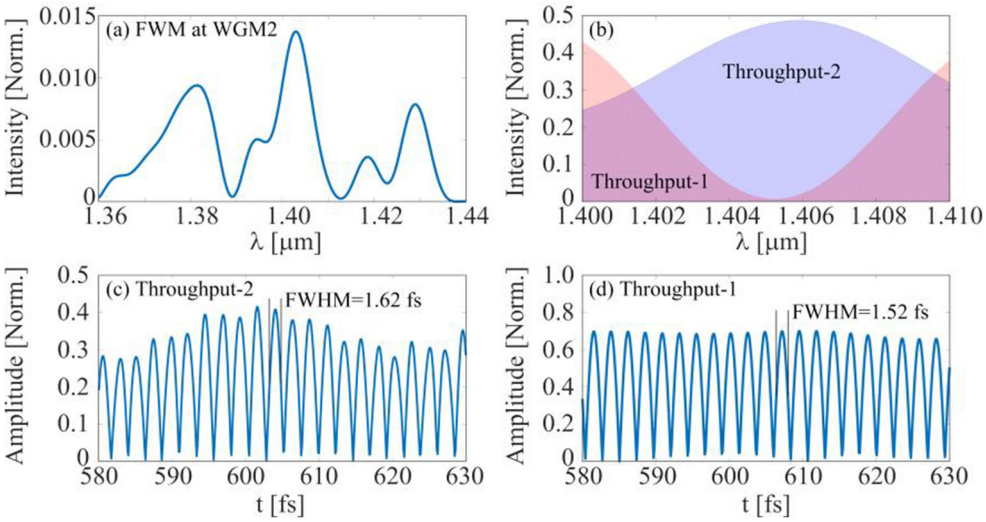


**Fig. 7** The simulation result of MATLAB program, where (**a**) FWM result of WGM2, (**b**) dark at Th-1 and bright at Th-2, (**c**) Clock result of Th-2, (**d**) Clock result of Th-1

bright-dark soliton conversion signals and vice versa, which can be used to form the transmission clock. From which both multiplexing methods called synchronous and asynchronous schemes can be applied. Regarding the four-wave mixing principle, the high capacity quantum bits transmission can be formed by the high-density switching pulses generated by the ***GaAsInP*** ring. Both transmission links by wireless and cable transmission systems can connect to the WGM beam antenna and throughput port outputs, respectively. Furthermore, the state of the electron spins (up or down) within the gold grating surface can be configured and teleported by the proposed transmission link by using the polarization entangle photons to establish the teleport electron cloud on the plasmonic transducer. The other form of the time-energy function can also be applied and transmitted using the same system. For an instant, the telepathic signal is a coherent wave of time-energy function that can be applied to the plasmonic transducer, multiplexed, and transmitted via the system, where telepathic communication (telephone) may be possible.

## Conclusion

We have proposed the use of the space-time function to accommodate the physical interpretation of waves in the silicon microring circuits. In manipulation, the relationship between the input power and Bragg wavelength is investigated for the possibility of using as the pressure wave transducer. The induced change in the Bragg wavelengths (signals) was

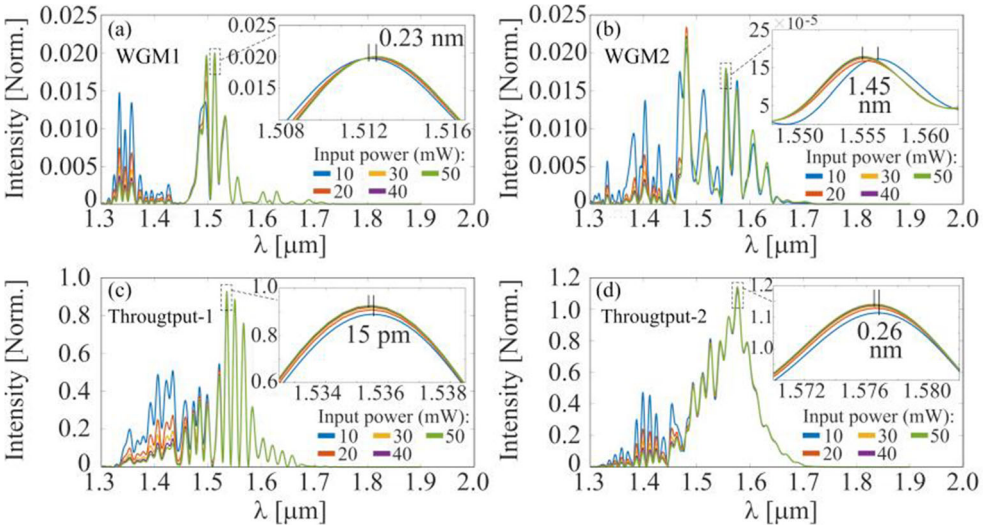


**Fig. 8** The plot results obtained by the MATLAB program, where (**a**) WGM1, (**b**) WGM2, (**c**) Throughput-1, and (**d**) Throughput-2, with the changes in input soliton power for sensor investigation

multiplexed to the quantum codes and clock, which was modulated by time function carrier for transmission. The transmission system can be employed by LiFi or cable transmission schemes. The downstream can be applied correspondingly. The filtering and de-multiplexing devices are included, from which the required information was obtained. In application, the potential of applications such as synchronous and asynchronous multiplexing, quantum security, LiFi, cable transmission, and electro-optic sensing transducer can be employed. Moreover, the feasibility of using the proposed design for a telepathic telephone link may be possible, where the spiritual energy is modeled as a time-energy function and then can also be applied.

**Acknowledgments** The authors would like to acknowledge the research facilities from the Ton Duc Thang University, Vietnam, and Rajamangala University of Technology Phra Nakhon, Bangkok 10300, Thailand.

## References

1. Youplao P, Pornsuwancharoen N, Amiri IS, Jalil MA, Aziz MS, Ali J, Singh G, Yupapin P, Grattan KTV (2018) Microring stereon sensors model using Kerr-Vernier effect for bio-cel sensor and communication. Nano Commun Netw 17:30–35
2. Koos C, Jacome L, Poulton C, Leuthold J, Freude W (2007) Nonlinear silicon-on-insulator waveguides for all-optical signal processing. Opt Express 15:5976–5990
3. Pornsuwancharoen N, Amiri IS, Suhailin FH, Aziz MS, Ali J, Singh G, Yupapin P (2017) Micro-current source generated by a WGM of light within a stacked silicon-graphene-Au waveguide. IEEE Photon Technol Lett 29(21):1768–1771
4. Xin HM, Huang YQ, Chen HB, Huang H, Ren X, Zhou XG (2009) Design and fabrication of InP micro-ring resonant detectors. Optoelectron Lett 5:6–10
5. Bogaerts W, de Heyn P, van Vaerenbergh T, de Vos K, Kumar Selvaraja S, Claes T, Dumon P, Bienstman P, van Thourhout D, Baets R (2012) Silicon micro-ring resonators. Laser Photon Rev 6(1):47–73
6. Atabaki AH, Moazeni S, Pavanello F, Gevorgyan H, Notaros J, Alloatti L, Wade MT, Sun C, Kruger SA, Meng H, al Qubaisi K, Wang I, Zhang B, Khilo A, Baiocco CV, Popović MA, Stojanović VM, Ram RJ (2018) Integrating photonics with silicon nanoelectronics for next generation of system on a chip. Nature 556:349–354
7. Dutt A, Luke K, Manipatruni S, Gaeta AL, Nussenzveig P, Lipson M (2015) On-chip optical squeezing. Phys Rev App 3:044005
8. Ali J, Pornsuwancharoen N, Youplao P, Aziz MS, Amiri IS, Chaiwong K, Chiangga S, Singh G, Yupapin P (2018) Coherent light squeezing states within a modified microring system. Results Phys 9:211–214
9. Youplao P, Sarapat N, Porsuwancharoen N, Chaiwong K, Jalil MA, Amiri IS, Ali J, Aziz MS, Chiangga S, Singh G, Yupapin P, Grattan KTV (2018) Plasmonic op-amp circuit model using inline successive microring pumping technique. Microsyst Technol 24(9):3689–3695
10. Ali J, Youplao P, Pornsuwancharoen N, Jalil MA, Chiangga S, Amiri IS, Punthawanunt S, Aziz MS, Singh G, Yupapin P, Grattan KTV (2018) Nano-capacitor-like model using light trapping in plasmonic island embedded microring system. Results Phys 10:727–730
11. Chaiwong K et al (2016) Four-wave mixing (FWM) effects within a micro-optical device. Int J Electron Electr Eng 4(3):1–4
12. Derkachova A, Kolwas K (2007) Size dependence of multipolar plasmon resonance frequencies and damping rates in simple metal spherical nanoparticles. Eur Phys J-Spec Top 144:93–99
13. Soysouvanh S, Jalil MA, Amiri IS, Ali J, Singh G, Mitatha S, Yupapin P, Grattan KTV, Yoshida M (2018) Ultra-fast electro-optic switching control using a soliton pulse within a modified add-drop multiplexer. Microsyst Technol 24(9):3777–3782
14. Sarapat N, Pornsuwancharoen N, Youplao P, Amiri IS, Jalil MA, Ali J, Singh G, Yupapin P, Grattan KTV (2019) LiFi up-downlink conversion node model generated by inline successive optical pumping. Microsyst Technol 25(3):945–950
15. Punthawanunt S, Yupapin P (2018) Meditation on a daily basis makes wise without violence. J Yoga Phys 4:555631
16. Lee TK, Kim HS, Oh GY, Lee BH, Kim DG, Chung TK, McCloskey D, Donegan JF, Choi YW (2014) Systematic analysis of whispering-gallery modes in planar silicon nitride microdisks. Opt Commun 322:188–197
17. Cai L, Pan J, Hu S (2020) Overview of the coupling methods used in whispering gallery mode resonator systems for sensing. Opt Lasers Eng 127:105968
18. Agrawal GP (2011) Nonlinear fiber optics: its history and recent progress. J Opt Soc Am B 28(12):A1–A10
19. Phatharaworamet T, Teeka C, Jomtarak R, Mitatha S, Yupapin PP (2010) Random binary code generation using dark-bright soliton conversion control within a panda ring resonator. IEEE Lightwave Technol 28(19):2804–2809
20. Tunsiri S, Thammawongsa N, Threepak T, Mitatha S, Yupapin P (2019) Microring switching control using plasmonic ring resonator circuits for super-channel use. Plasmonics 14:1669–1677
21. Wolpert DH, Kolchinsky A, Owen JA (2019) A space-time tradeoff for implementing a function with mater equation dynamics. Nat Commun 10:1727
22. Yessenov M, Bhaduri B, Kondakci HE, Abouraddy AF (2019) Weaving the rainbow: space-time optical wave packets. Opt Photon News 30(5):34–41
23. Yee KS (1966) Numerical solution of initial boundary value problems involving Maxwell's equations in isotropic media. IEEE Trans Antennas Propag 51:302–307
24. Silverstone JW, Santagati R, Bonneau D, Strain MJ, Sorel M, O'Brien JL, Thompson MG (2015) Qubit entanglement between ring-resonator photon pair sources on a silicon chip. Nat Commun 6:7948